Supramolecular Copolymerization as a Strategy to Control the Stability of Self-Assembled Nanofibers

Supramolecular copolymerization as a strategy to control the stability of self-assembled nanofibers

B. Thota,[1,2] X. Lou,[1] D. Bochicchio,[3] T. F. E. Paffen,[1] R. P. M. Lafleur,[1] J. L. J. van Dongen,[1] R. Haag,[2] G. M. Pavan,[3] A. R. A. Palmans,[1] E. W. Meijer.[1]

[1] *Institute for Complex Molecular Systems and Laboratory of Macromolecular and Organic Chemistry, Eindhoven University of Technology, 5612 AZ Eindhoven, The Netherlands*

[2] *Institute of Chemistry and Biochemistry, Freie Universität Berlin, Berlin 14195, Germany*

[3] *Department of Innovative Technologies, University of Applied Sciences and Arts of Southern Switzerland, Galleria 2, CH-6928 Manno, Switzerland*

ABSTRACT: *One of the major challenges to be addressed in supramolecular polymerizations is the ability to control the stability of the polymers formed, i.e. to control the rate of monomer exchange in the equilibrium between monomer and polymer. We here show that the exchange dynamics of supramolecular polymers based on the benzene-1,3,5-tricarboxamide (BTA) motif can be regulated by copolymerizing molecules with dendronized (**dBTA**) and linear (**nBTA**) ethylene glycol-based water-soluble side chains. Whereas **nBTAs** form long nanofibers in water, **dBTAs** do not polymerize and form small aggregates only. In contrast, the copolymerization of the two BTAs results in long nanofibers up to an equimolar ratio of both components. Intriguingly, the exchange dynamics of both the BTA monomers in the copolymer are significantly slowed down in the mixed systems, leading to a more stable copolymer, while the morphology and spectroscopic signature of the copolymers are identical to that of the homopolymer of **nBTA**. In many ways, this copolymerization represents the supramolecular counterpart of the copolymerization of styrene and maleic anhydride.*

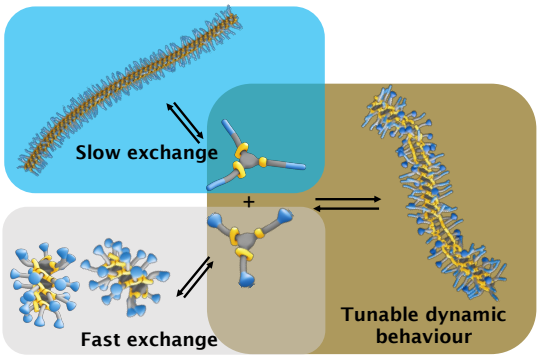

Multicomponent self-assembly is a unique strategy in the development of functional supramolecular systems, as it provides ways to tune the physical behavior of these systems.[1–6] Introducing such a concept in the area of supramolecular polymers will expand their potential in applications and demonstrate the advantage of a modular, non-covalent synthetic approach.[7–10] In the last two decades, these supramolecular polymers have been extensively studied to understand the mechanisms behind their polymerization process,[11] with the aim to develop new motifs that could result in polymers with superior properties. Also significant progress has been made in the area of supramolecular copolymerizations to control the microstructure of the copolymers formed.[12–15] A major challenge to be addressed in these supramolecular copolymers is the ability to control their stability and/or dynamic behavior in the equilibrium exchange dynamics between monomers and polymers.[16–20] In addition, it will unveil the similarities and differences between supramolecular polymers and their covalent macromolecular counterparts.

In classical covalent copolymer formation, in which the copolymerization of different monomers results in random, block, gradient or precision copolymers, the copolymer properties can be accurately tuned by tuning the reactivity ratios of the monomers in combination with advanced polymerization methods.[21–23] An intriguing example is the copolymerization of styrene with maleic anhydride. The latter does not polymerize, but when copolymerized with styrene, a very stable – high T_g – copolymer is obtained. We envisage that in the supramolecular counterpart, i.e. copolymerizing supramolecular monomers with distinct differences in the dynamic behavior of and steric demands in their respective aggregates could provide a handle to control the overall exchange dynamics of the supramolecular copolymer as well, and hereby their stability and applicability.

Herein, we report the supramolecular copolymerization of two benzene-1,3,5-tricarboxamide-based molecules (**nBTA** and **dBTA**, Scheme 1), of which **dBTA** is unable to polymerize on its own. We apply hydrogen-deuterium exchange mass spectrometry (HDX-MS) to monitor the exchange dynamics of supramolecular polymers and copolymers, as it has recently been proved to be a powerful label-free method to elucidate dynamic processes in supramolecular polymers.[24] Remarkably, the exchange dynamics of both monomers are slowed down upon copolymerization, a results that is seconded by molecular dynamics simulations.

All BTAs were synthesized according to standard procedures.[25–27] The synthetic details and molecular characterization of newly synthesized **dBTA**, **d1BTA** and **d2BTA** are given in the

Supporting Information (Figures S1-9). The supramolecular polymerization of **nBTA** in water has been well documented and is typically studied by spectroscopic (UV-vis and FT-IR), microscopic (cryogenic transmission electron microscopy, cryoTEM) and scattering techniques (dynamic light scattering, DLS, and small angle X-ray scattering, SAXS) in combination with molecular dynamics simulation studies and HDX-MS exchange dynamics.[24,28–31]

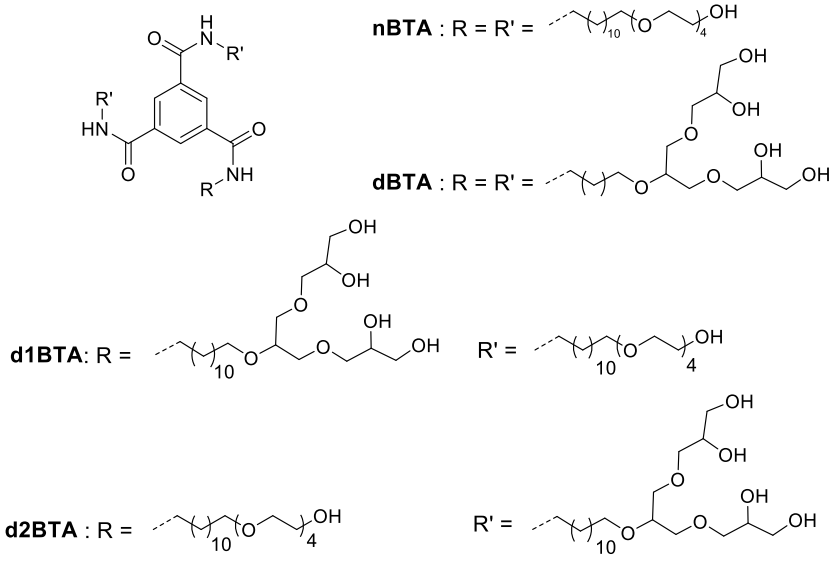

Scheme 1. Chemical structures of the BTA derivatives applied in this work.

The formation of supramolecular polymers stabilized by intermolecular hydrogen bonding of **nBTA** in water is characterized by two absorption maxima at 211 nm and 228 nm in the UV spectrum.[30] In contrast, when molecularly dissolved, **nBTA** shows one maximum at 204 nm.[27] The formation of intermolecular hydrogen bonds between the amides at the BTA core in water is evidenced by a shift in the amide I band from 1648 cm^{-1} in MeOH-*d4* to 1635 cm^{-1} in D_2O. The dendritic **dBTA** displays a different absorption spectrum with a maximum at 197 nm (Figure 1A). At higher concentrations, the FT-IR spectrum of **dBTA** does resemble that of **nBTA** in water (Figure 1B). CryoTEM analysis of **nBTA** shows the formation of one-dimensional nanofibers (Figure S10), while no conclusive cryoTEM images of **dBTA** could be obtained. Additional TEM measurements of **dBTA** suggest the formation of small spherical aggregates (Figure S11), which was corroborated by DLS measurements showing particle sizes of around 10 nm (Figure S12). Thus, whereas **nBTA** homopolymerizes in water into long cylindrical aggregates, **dBTA** is unable to do so.

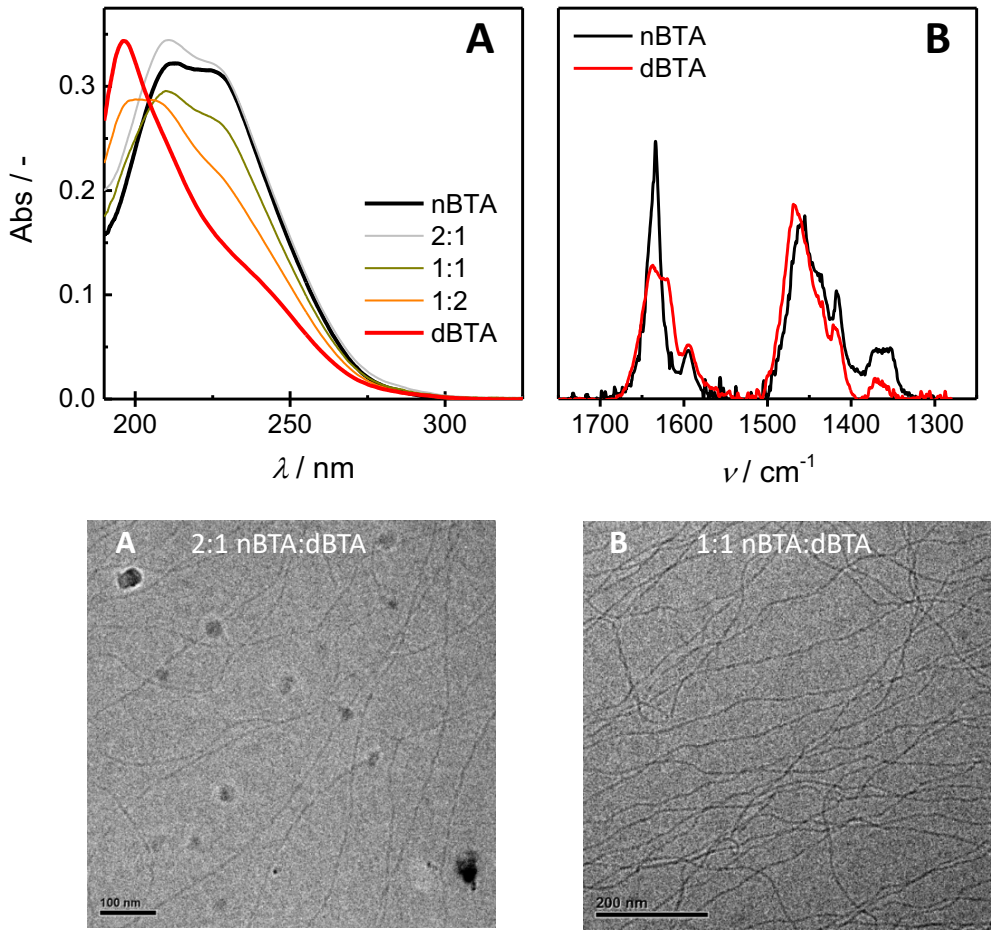

Figure 1. A) UV-vis spectra of **nBTA** and **dBTA** homo- and copolymers in water at c_{BTA} = 100 μM (path length = 1 mm). B) FT-IR spectra of **nBTA** and **dBTA** in D_2O at at c_{BTA} = 25 mg mL^{-1} (corresponding to 19.4 mM for **nBTA** and 16.8 mM for **dBTA**). C) CryoTEM of a 2:1 mixture of **nBTA** and **dBTA** measured at c_{BTA} = 1 mM, scale bar = 100 nm; D) CryoTEM of a 1:1 mixture of **nBTA** and **dBTA** measured at c_{BTA} = 1 mM, scale bar = 200 nm.

In a next step, the supramolecular copolymerization of **nBTA** and **dBTA** was investigated at different mixing ratios. UV-vis spectra of these mixtures resulted in absorption spectra similar to **nBTA** up to a mixing ratio of 1:1 (Figure 1A). Above 50 mol% of **dBTA** present in the mixtures, a UV spectrum different from the parent molecules was observed. This observations suggests that up to a 1:1 ratio, the organization of hydrogen bonds within the supramolecular copolymers of **nBTA** and **dBTA** is similar to that of pure **nBTA**. The morphology of the supramolecular copolymers measured through electron microscopy experiments corroborated this; cryoTEM images indicated the formation of nanofibers similar to **nBTA** polymer for both 2:1 and 1:1 mixtures of **nBTA** and **dBTA** (Figure 1C-D). Although the

cryoTEM of the 1:2 mixture did not show any fibers, TEM imaging of the solution revealed the presence of shorter fibers and small aggregates (Figure S11).

Monomers **d1BTA**, with one dendritic wedge, and **d2BTA** with two dendritic wedges, are the perfect comparison to the copolymers with 2:1 and 1:2 ratio of **nBTAs** and **dBTAs**. Whereas **d1BTA** showed a UV spectrum similar to **nBTA**, **d2BTA** displayed a similar UV profile as that of **dBTA** (Figure S13). The new analogs are not only similar in their spectroscopic signature to **nBTA** and **dBTA**, but their morphologies are also similar; **d1BTA** results in a 1D nanofiber and **d2BTA** gives smaller aggregates as evidenced by TEM measurements (Figure S14).

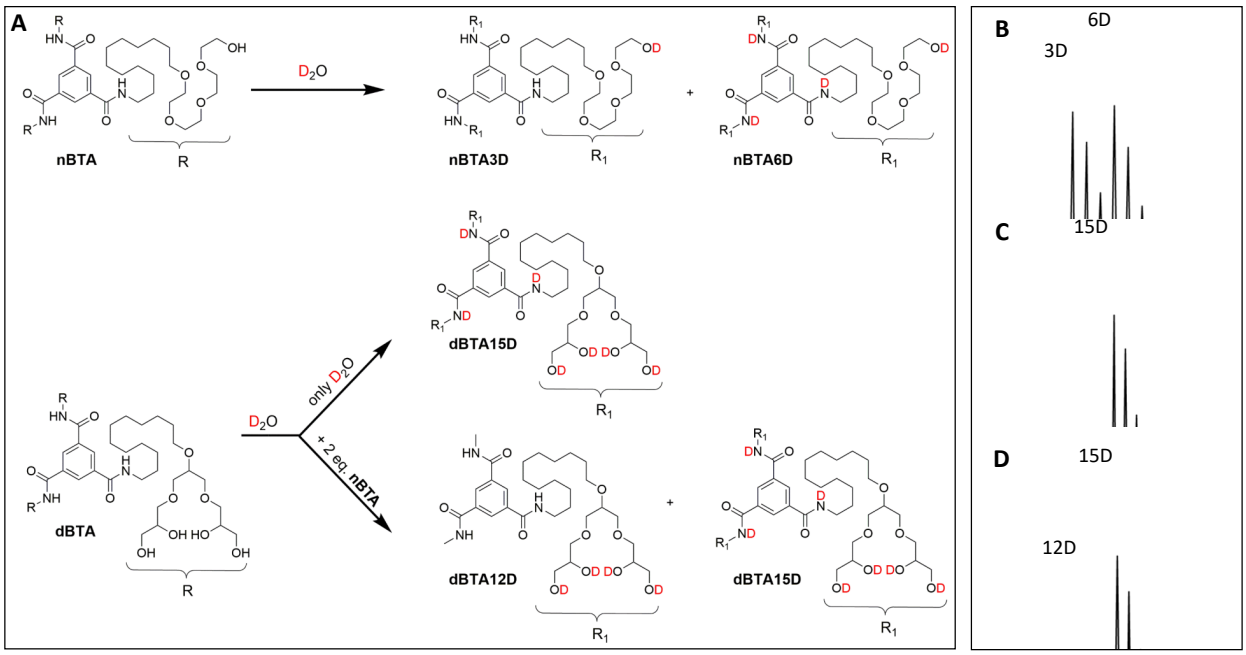

Figure *2.* A) HDX of **nBTA** or **dBTA** after dilution in D_2O in which either only OH is replaced by OD or also NH is replaced to ND. B) ESI-MS of **nBTA** taken after 1 h shows two isotopic distributions corresponding to **nBTA3D** and **nBTA6D**. C) ESI-MS of **dBTA** taken after 3 min shows only one isotopic distribution corresponding to **dBTA15D**. D) ESI-MS of **dBTA** of a 2:1 mixture of **nBTA** and **dBTA** taken after 1 h shows two isotopic distributions corresponding to **dBTA12D** and **dBTA15D**.

Next we performed HDX-MS experiments to compare the exchange dynamics of both the individual aggregates with those of the copolymers. Hereto, 500 µM solutions of **nBTA, dBTA,** or mixtures thereof were prepared in water and 100 times diluted in D_2O (Figure 2A). Upon dilution, the nature of the aggregates did not change (Figure S15). Figure 2B shows the ESI-MS

spectrum of **nBTA** taken 1 h after dilution in D_2O. Two populations in the isotope distributions can be distinguished, one corresponding to three times deuterated species (**nBTA3D**) and one corresponding to six times deuterated species (**nBTA6D**). In contrast, dilution of **dBTA** into D_2O shows the presence of only one isotopic distribution that corresponds to a mass increase of 15 units (**dBTA15D**) immediately after diluting (Figure 2C). The significant differences in morphologies formed by **nBTA** and **dBTA** are therefore also reflected in the H/D exchange rates of the amide protons. HDX-MS experiments on a 2:1 mixture of **nBTA** and **dBTA** by the same protocol (Figure 2D) after 1 h showed, surprisingly, the presence of the isotopic mass distribution of **dBTA12D** (Figure 2C), indicative that the amide protons in **dBTAs** are, at least to a certain degree, hydrophobically shielded from the surrounding water in the supramolecular copolymer.

More quantitative data were collected from kinetic measurements of the HDX-MS experiments (Figure 3A and 3B, 1:1 mixture, red data points). Immediately after dilution of the solutions in D_2O, the percentages of both **nBTA3D** and **dBTA12D** are 100%, since all OH are instantaneously exchange to OD. When in time NH exchanges to ND, the percentage of **nBTA3D** and **dBTA12D** decreases. By quantifying the intensities of the **dBTA12D** and **nBTA3D** isotope peaks as a function of time, we observe very fast decreases in the first hour which slow down significantly afterwards. Strikingly, we notice that the mass spectra of **nBTA** show that **nBTA3D** species are more abundant in the 1:1 mixture compared to pure **nBTA** (Figure 3A, black data points). This indicates that fewer amides are exposed to the surrounding water and as a result, the monomers are more stably incorporated into the supramolecular copolymers of the 1:1 mixture.

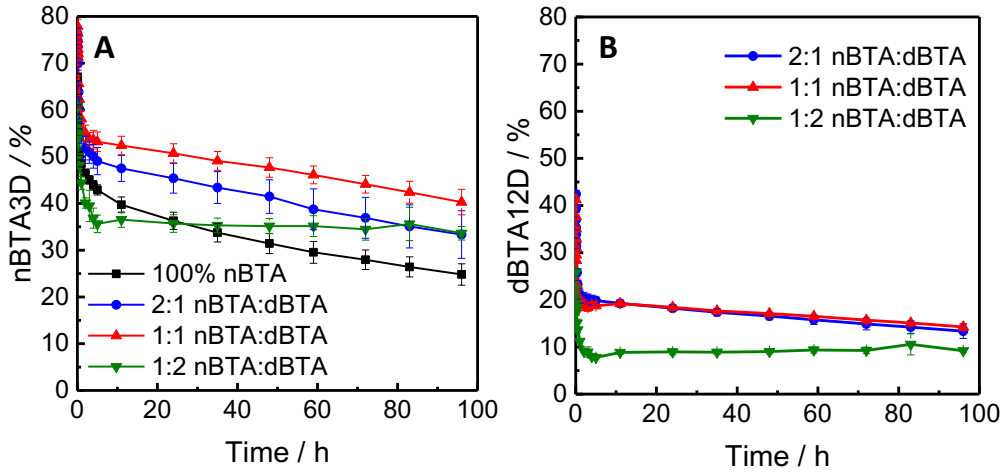

Figure 3. HDX-MS of **nBTA**, **dBTA** and their mixtures followed as a function of time in which the percentage of A) **nBTA3D** or B) **dBTA12D** is probed.

HDX-MS experiments were conducted also for higher and lower **nBTA**:**dBTA** ratios as a function of time (Figure 3A,B). At 2:1 and 1:1 **nBTA**:**dBTA**, the copolymers showed higher percentages of remaining **nBTA3D** compared to the homopolymer of **nBTA**, which indicates a higher shielding/ordering of the amides and therefore decrease in dynamics. At 1:2 **nBTA**:**dBTA** ratio, however, **nBTA** displayed a considerably faster decay at the early phase of the measurement, and slowed down dramatically after a few hours after which the percentage of **nBTA3D** remained almost constant. A similar trend was also observed for the decay of **dBTA12D**. A more quantitative approach to elucidate the dynamic features of the copolymers was performed by fitting the decay data by a tri-exponential fit (see Supporting Information for details). The fits clearly indicate three distinct decay processes that occur in these systems with different rate constants ($k_{initial}$, k_{fast} and k_{slow}, Table S1, Figure S16). The results unambiguously show an increase in the fraction of the slowest exchange process with the **dBTA:nBTA** ratio up to 1:1, at the expense of the fastest one, indicating an increase in the stability of the copolymer nanofibers. Similar trends are also observed for **dBTA** data (Table S2, Figure S16). All the HDX experiments indicate the formation of an increase in the stability of the supramolecular copolymers compared to the homopolymers.

Also the supramolecular polymers of the **d1BTA** and **d2BTA**-based aggregates were analyzed (Figure S17). Polymers of **d1BTA** show a similar decay curve as that obtained for the **nBTA** polymers. In contrast, H-D exchange for all OH and NH protons occurred instantaneously

in case of **d2BTA**, which is identical to the results obtained for **dBTA**. Although the molecular composition of **d1BTA** is comparable to the composition of copolymers of **nBTA** and **dBTA** with 2:1 and 1:2 ratio, respectively, their dynamic behavior is not. The most pronounced difference is present between **d2BTA** – showing instantaneous H/D exchange – and the 2:1 **dBTA**/**nBTA** mixture in which complete exchange takes days. An interesting next question will answer if it is possible to capture any structural difference between an **nBTA**:**dBTA** copolymer and a **nBTA** polymer capable to explain such a dynamic difference at a molecular level.

To help answering this, we performed all-atom molecular dynamics (MD) simulations on a copolymer composed of a mixture of **nBTA**:**dBTA** in a 2:1 ratio (Figure 4A). For details of the method, the reader is referred to the Supporting Information. Our earlier simulation studies indicated the fibers are not perfect and extended in water, but undergo folding due to hydrophobic effects to shield the interaction between the hydrophobic parts of the structure with water. Such folding produces a level of disorder [17,29] and the radial distribution function (*g(r)*) between the monomer cores as a function of the inter-core distances provides an indication of the level of stacking order in the polymers.[17,29,31,32] Higher *g(c)* peaks (relative probability for finding cores at stacking distance c = 3.4 Å from the neighbors) indicate higher persistence/regularity of the stacking. The *g(r)* of the cores was extracted from the equilibrated phase MD trajectory of the 2:1 **nBTA**:**dBTA** copolymer (last 100 ns of MD simulation) and compared to that obtained for **nBTA** (Figure 4B).[29,31] A higher persistence/order (~15%) of the core-core stacking in the equilibrated copolymer compared to **nBTA** homopolymer is observed. Moreover, we calculated the *g(r)* between the **nBTA** cores and water (probability of finding water molecules as a function of the distance between the **nBTA** cores) from the MD simulations (Figure 4C). This data show that the level of hydration of the cores is reduced in the copolymer compared to the **nBTA** homopolymer (less contacts between cores and water molecules).

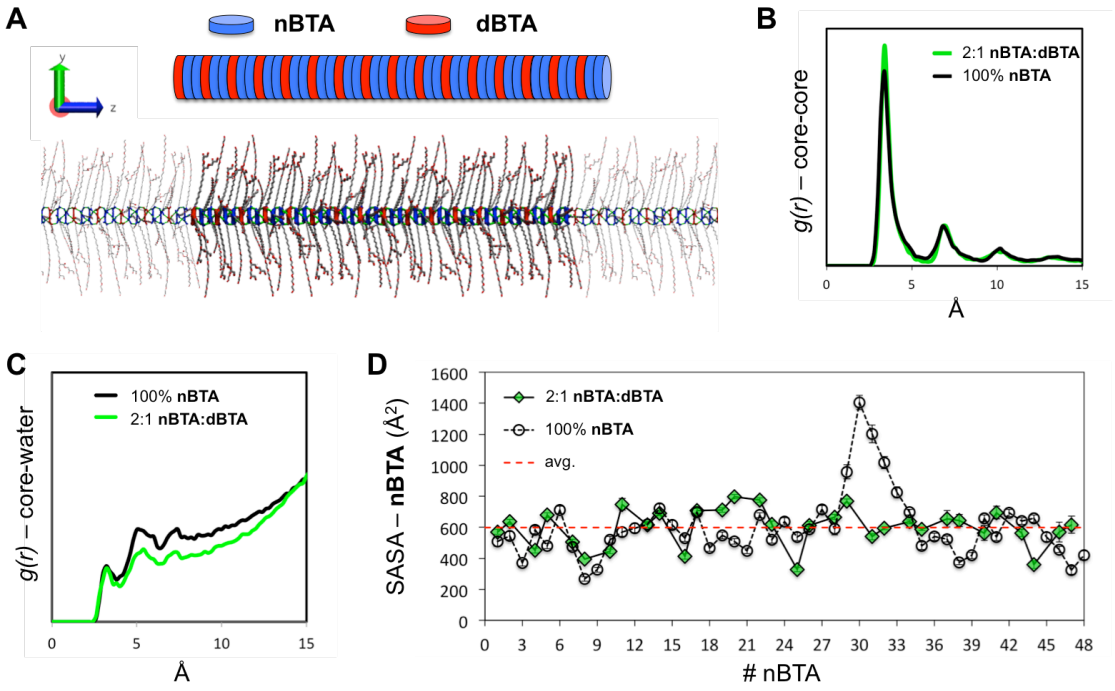

Figure 4: All-atom molecular dynamics (MD) simulations. (A) Initial configuration for the 2:1 **nBTA**:**dBTA** copolymer, which was then relaxed and equilibrated in water. (B) Core-core radial distribution functions (*g(r)*) for the **nBTA** homopolymer (black) and the 2:1 **nBTA**:**dBTA** copolymer (green). (C) Core-water radial distribution functions (*g(r)*) in the **nBTA** homopolymer (black) and 2:1 **nBTA**:**dBTA** copolymer (green). (D) Solvent accessible surface area (SASA) for the **nBTA** monomers in the **nBTA** homopolymer (black) and 2:1 **nBTA**:**dBTA** copolymer (green). The average for **nBTA** monomers in the assemblies is identified in red.

Next, we analyzed the solvent-accessible surface area (SASA) of the BTAs within the fibers. As seen in Figure 4D, the SASA data for the **nBTA** monomers in the copolymer (green) are uniformly distributed round the average (red line) different from those in the homopolymer (black), where at least one large defected domain is evidenced in our fiber model (*i.e.*, in a fiber section of 48 monomers). [17] This suggests that the incorporation of **dBTA** monomers, with their larger surface, into the copolymer improves the regularity in the monomer-monomer packing and reduces the probability of creating defects (exchange hot spots) along the fiber, which fits well with the reduced **nBTA** exchange dynamics seen experimentally in these copolymers.

In conclusion, the morphologies and dynamic behavior of supramolecular homo- and copolymers based on **nBTA** and **dBTA** were investigated. The supramolecular copolymerization of **nBTA** and **dBTA** up to a 1:1 ratio afforded nanofibers with the same spectroscopic signature and morphology as that of **nBTA,** but significantly reduced exchange behavior of the monomers

in the copolymer as compared to the individual aggregates. Molecular dynamics simulations performed on a 2.1 **nBTA**:**dBTA** copolymer revealed that the degree of order between monomers in the supramolecular polymer was increased when **dBTA** monomers were added to a **nBTA** homopolymer. This increase in order was corroborated by a decreased tendency to form discontinuity points/defects that may work as "exchange hot spots", which likely decreases the exchange dynamics of nanofibers. As this study shows a behavior similar to what is reported on the covalent styrene - maleic anhydride co-polymerization, it illustrates remarkable and unforeseen similarities between macromolecules and supramolecular polymers.

Acknowledgments

The authors acknowledge financial support from the Dutch Ministry of Education, Culture and Science (Gravity program 024.001.035). G.M.P. acknowledges the support from the Swiss National Science Foundation (SNSF grant 200021_162827), and B.T. and R.H. ….. the …. E.W.M. thanks the Humboldt Foundation for support. The authors gratefully acknowledge Sandra Schoenmakers for assisting with UV measurements.

References

[1] E. Krieg, M. M. C. Bastings, P. Besenius, B. Rybtchinski, *Chem. Rev.* **2016**, *116*, 2414–2477.

[2] C. J. C. Edwards-Gayle, I. W. Hamley, *Org. Biomol. Chem.* **2017**, *15*, 5867–5876.

[3] R. V Ulijn, A. M. Smith, *Chem. Soc. Rev.* **2008**, *37*, 664.

[4] P. Y. W. Dankers, E. W. Meijer, *Bull. Chem. Soc. Jpn.* **2007**, *80*, 2047–2073.

[5] O. J. G. M. Goor, S. I. S. Hendrikse, P. Y. W. Dankers, E. W. Meijer, *Chem. Soc. Rev.* **2017**, *46*, 6621–6637.

[6] T. Aida, E. W. Meijer, S. I. Stupp, *Science (80-.).* **2012**, *335*, 813–817.

[7] H. Frisch, J. P. Unsleber, D. Lüdeker, M. Peterlechner, G. Brunklaus, M. Waller, P. Besenius, *Angew. Chemie Int. Ed.* **2013**, *52*, 10097–10101.

[8] H. Frisch, Y. Nie, S. Raunser, P. Besenius, *Chem. - A Eur. J.* **2015**, *21*, 3304–3309.

[9] H. Frisch, E.-C. Fritz, F. Stricker, L. Schmüser, D. Spitzer, T. Weidner, B. J. Ravoo, P. Besenius, *Angew. Chemie Int. Ed.* **2016**, *55*, 7242–7246.

[10] P. Besenius, *J. Polym. Sci. Part A Polym. Chem.* **2017**, *55*, 34–78.

[11] T. F. A. De Greef, M. M. J. Smulders, M. Wolffs, A. P. H. J. Schenning, R. P. Sijbesma, E. W. Meijer, *Chem. Rev.* **2009**, *109*, 5687–5754.

[12] W. Zhang, W. Jin, T. Fukushima, A. Saeki, S. Seki, T. Aida, *Science (80-.).* **2011**, *334*, 340–343.

[13] D. Görl, X. Zhang, V. Stepanenko, F. Würthner, *Nat. Commun.* **2015**, *6*, 7009.

[14] H. Qiu, Z. M. Hudson, M. A. Winnik, I. Manners, *Science (80-.).* **2015**, *347*, 1329–1332.

[15] A. Das, G. Vantomme, A. J. Markvoort, H. M. M. Ten Eikelder, M. Garcia-Iglesias, A. R. A. Palmans, E. W. Meijer, *J. Am. Chem. Soc.* **2017**, *139*, 7036–7044.

[16] L. Albertazzi, D. van der Zwaag, C. M. A. Leenders, R. Fitzner, R. W. van der Hofstad, E. W. Meijer, *Science (80-.).* **2014**, *344*, 491–495.

[17] D. Bochicchio, M. Salvalaglio, G. M. Pavan, *Nat. Commun.* **2017**, *8*, 147.

[18] P. Ahlers, K. Fischer, D. Spitzer, P. Besenius, *Macromolecules* **2017**, *50*, 7712–7720.

[19] J. H. Ortony, C. J. Newcomb, J. B. Matson, L. C. Palmer, P. E. Doan, B. M. Hoffman, S. I. Stupp, *Nat. Mater.* **2014**, *13*, 812–816.

[20] R. M. P. da Silva, D. van der Zwaag, L. Albertazzi, S. S. Lee, E. W. Meijer, S. I. Stupp, *Nat. Commun.* **2016**, *7*, 11561.

[21] P. B. Zetterlund, S. C. Thickett, S. Perrier, E. Bourgeat-Lami, M. Lansalot, *Chem. Rev.* **2015**, *115*, 9745–9800.

[22] J.-F. Lutz, J.-M. Lehn, E. W. Meijer, K. Matyjaszewski, *Nat. Rev. Mater.* **2016**, *1*, 16024.

[23] M. Chen, M. Zhong, J. A. Johnson, *Chem. Rev.* **2016**, *116*, 10167–10211.

[24] X. Lou, R. P. M. Lafleur, C. M. A. Leenders, S. M. C. Schoenmakers, N. M. Matsumoto, M. B. Baker, J. L. J. van Dongen, A. R. A. Palmans, E. W. Meijer, *Nat. Commun.* **2017**, *8*, 15420.

[25] M. Wyszogrodzka, R. Haag, *Chem. - A Eur. J.* **2008**, *14*, 9202–9214.

[26] M. L. Ślęczkowski, E. W. Meijer, A. R. A. Palmans, *Macromol. Rapid Commun.* **2017**, 1700566.

[27] C. M. A. Leenders, L. Albertazzi, T. Mes, M. M. E. Koenigs, A. R. A. Palmans, E. W. Meijer, *Chem. Commun.* **2013**, *49*, 1963.

[28] L. Albertazzi, F. J. Martinez-Veracoechea, C. M. A. Leenders, I. K. Voets, D. Frenkel, E. W. Meijer, *Proc. Natl. Acad. Sci.* **2013**, *110*, 12203–12208.

[29] M. B. Baker, L. Albertazzi, I. K. Voets, C. M. A. Leenders, A. R. A. Palmans, G. M.

Pavan, E. W. Meijer, *Nat. Commun.* **2015**, *6*, 6234.

[30] C. M. A. Leenders, M. B. Baker, I. A. B. Pijpers, R. P. M. Lafleur, L. Albertazzi, A. R. A. Palmans, E. W. Meijer, *Soft Matter* **2016**, *12*, 2887–2893.

[31] M. Garzoni, M. B. Baker, C. M. A. Leenders, I. K. Voets, L. Albertazzi, A. R. A. Palmans, E. W. Meijer, G. M. Pavan, *J. Am. Chem. Soc.* **2016**, *138*, 13985–13995.

[32] D. Bochicchio, G. M. Pavan, *ACS Nano* **2017**, *11*, 1000–1011.